



MRP-Net: Seizure detection method based on modified recurrence plot and additive attention convolution neural network

Wenkai Huang*, Haizhou Xu, Yujia Yu

School of Mechanical and Electrical Engineering, Guangzhou University, Guangzhou 510006, China

ARTICLE INFO

Keywords:

Electroencephalogram (EEG)
Modified recurrence plot
Epileptic seizure
Phase space
Deep learning
Additive attention

ABSTRACT

Electroencephalographic (EEG) signals play an important role in the detection of seizures in epilepsy, and accurate detection of seizures can buy patients valuable treatment time. However, most seizure detection methods ignore the nonlinear, implicit characteristics of EEG, which has some impact on the accuracy of detection. Therefore, in this paper, we propose an EEG epilepsy detection network (MRP-Net) based on modified recurrence plot (MRP) and additive attention convolution neural network. This network can fully take into account the nonlinear, occult characteristics of EEG which can be mapped to the two-dimensional plane and served as the input of additive attention convolution neural network to automatically learn, analyze, and extract the EEG characteristics of seizures. The performance of the proposed method was evaluated on the Bonn University dataset and the SWEC-ETHZ short-term dataset. Sensitivity, specificity and accuracy were 100% in multiple detection tasks in the University of Bonn single-channel EEG dataset. The sensitivity, specificity and accuracy of SWEC's short-term, multi-channel EEG dataset were 99.77%, 99.57% and 99.69%, respectively, higher than the latest methods (3.76%, 4.73% and 4.27%). The results of the experiments show that the network in this paper is superior and universal in epilepsy detection.

1. Introduction

Epilepsy is a chronic brain disorder caused by excessive neuronal discharges in the brain. Accurate detection and treatment of seizure phenomena in patients with epilepsy can effectively reduce the high risk of harm caused by seizures [1]. The EEG signal contains a rich and complex signal of activity in the brain, and detection of the presence of repetitive neural discharges by observing the patient's EEG signal is the standard technique for diagnosing seizures in current clinical practice; however, in traditional clinical practice, seizure detection is a demanding process, and the whole EEG data is usually analyzed in detail by trained neurologists to determine the characteristic pattern of the disease [2]. At the same time, epilepsy is a highly nonstationary manifestation with variability not only between patients but even within the same patient, whose own multiple seizures vary widely. Thus, how to automatically and accurately detect seizures is the key to treating epileptic disorders.

Before this paper, many epileptic EEG feature extraction algorithms and automatic seizure detection algorithms have been in place. Kumar et al. [3] use one-dimensional local binary pattern (1D-LBP) to describe the EEG texture features of seizures and the nearest neighbor classifier utilizes the histogram matching scores was used to determine whether the acquired EEG signal belongs to seizure or seizure-free

category. Aydin et al. [4] apply LogEn to characterize the signal of EEG complexity and use a multilayer neural network for seizure detection. Ieracitano et al. [5] apply continuous wavelet transform (CWT) to each channel signal, and then the wavelet coherence coefficients of each channel are calculated to reflect the changes of EEG signals during seizures. The hierarchical clustering (HC) method is used to classify the ecology of EEG signals. Zhang and Chen [6] use the local mean decomposition (LMD) algorithm in the time–frequency domain, and the fusion features are input into support vector machine that is optimized by genetic algorithm (GA-SVM) for classification. Mursalin et al. [7] use an improved correlation-based feature-selection method to select the most prominent features from time domain, frequency domain, and entropy, and then they use random forest (RF) classifier to detect seizures. Literature [8] proposed a coherence function (CF) to analyze the EEG synchronization of intracortical EEG sequences recorded from rats in the case of anhedonic epilepsy, and compared the performance of different PSD predictors to calculate the crossover spectrum. Literature [9] uses the step-wise least square estimation algorithm (SLSA) to estimate Auto-Regressive (AR) models for normal and ictal EEG series, with SLSA providing the most descriptive order that can mark seizure. Literature [10,11] propose an epilepsy detection algorithm for each patient. The former uses harmonic wavelet packet

* Corresponding author.

E-mail address: smallkat@gzhu.edu.cn (W. Huang).

transform (HWPT) to obtain harmonic multiresolution from EEG and extract the self-similar fractal features of EEG to input to support vector machine (SVM) for detection, while the latter converts the EEG time series of each electrode into symbolic local binary pattern coding. The holographic distribution of brain states over time in all electrodes and hyperdimensional space is then constructed to detect seizures in people with epilepsy. Although many of the above studies have achieved some results, based on the traditional machine learning algorithm model for complex transformation data, its generalization ability is limited and based on the need for researchers to have a deep understanding of the physiological mechanism and clinical manifestations of epilepsy, relying on expert experience, deep features are not easy to be observed and extracted. Therefore, how to extract the most recognizable features from the EEG signals of patients with seizures and construct a model with strong generalization ability is the key to automatically and accurately detect seizures.

In recent years, thanks to the vigorous development of deep learning, which has shown great dynamism in the field of EEG epilepsy detection. Deep learning can learn high latitude abstract representation from natural signals [12] with better generalization performance. Acharya et al. [13] have applied deep learning to automatic epilepsy detection for the first time, and 13-layer deep convolution neural network (CNN) is used to detect epileptic activity. mei Hu et al. [14] have proposed a method of epilepsy detection based on deep, bidirectional, long-term and bi-directional long short-term model (Bi-LSTM) that can judge the current brain activity by analyzing the EEG information before and after the current moment. Zhao et al. [15] use correlation matrix to simulate the spatial relationship of EEG signals, and then they use linear graph convolution network (LGCN) to detect epilepsy. Woodbright et al. [16] directly input single-channel EEG data into CNN on Bonn University Dataset. Through the stack of two convolution layers and a maximum pool layer, abstract features of different levels are directly extracted from EEG. Finally, the prediction results are output through the full connection layer. Although deep learning models have stronger generalization learning ability and can reduce the reliance on manual features compared to traditional machine learning models, however, most of the current studies including those mentioned above tend to focus on the deep learning models themselves, skipping the manual feature extraction process and ignoring the intrinsic signal characteristics of EEG, which has some impact on the accuracy of detection.

The brain is a complex, nonlinear, dynamic system, and the EEG signal is nonlinear and nonstationary [17–19], indicating that the nonlinear characteristics of EEG play an important role in epilepsy detection. The current methods for nonlinear dynamics analysis of EEG signals include fractal dimension (FD) [20,21], Lyapunov index [22–24], Hurst index [25,26], entropy [27–29] and recurrence quantification analysis (RQA) [30–32]. Although the traditional nonlinear dynamics analysis methods can describe the nonlinear dynamics of different types of EEG signals, the computational complexity is high, and the corresponding computational time consumption increases significantly when the data length is long. In addition, the quantitative analysis method based on statistics is difficult to combine with the deep learning model with strong generalization ability. Recurrence plot [33], as a recently developed signal-processing tool for nonlinear, nonstationary signals not only characterizes the dynamical properties of their signals in the form of images with low computational complexity but also reflects the autocorrelation of signals on all their time scales and thus it can be easily combined with CNN to construct deep learning model. The nonlinear dynamic analysis method based on recurrence plot and CNN has been widely used in many fields, Wang et al. [34], the recurrence plot is used to extract the nonlinear dynamic characteristics from the fault signal of the planetary gear set, and then the shallow CNN is constructed to classify the recurrence plot. Ozkok and Celik [35], converted one of the products of the Real-time polymerase chain reaction (PCR), high-resolution melting (HRM), into a recurrence plot

and classified it with CNN. Meng et al. [36], proposed a new algorithm for EEG motion image classification, and the method based on recurrence plot and CNN showed promising results compared to previous studies.

Although recurrence plot combined with CNN have the above advantages and are widely used in various fields, they still have shortcomings that make them difficult to adapt to automatic EEG seizure detection: First, recurrence plot is only applicable to single-channel EEG data, and the choice of threshold value can make it lose nonlinear occlusion information. Second, EEG is essentially time series data, and the constructed recurrence plot has autocorrelation, while CNN has the field of view limitation, which makes it difficult to catch long-range feature autocorrelation. In light of the foregoing, we propose an epilepsy detection approach based on the modified recurrence plot (MRP) and an additive attention convolution neural network. By changing the phase space and recurrence plot construction, the MRP is adapted to multi-channel EEG data and retains richer nonlinear occultation features, and the additive attention convolution neural networks is proposed to capture long-range autocorrelation by adding additive attention in CNN to expand the field of view. The main contributions of this paper are as follows:

- A modified recurrence plot algorithm is proposed to extract the nonlinear dynamical features of EEG.
- An additive attention convolutional neural network module is designed to capture the long-range dependencies in recurrence plot and learn the autocorrelation of EEG signals.
- An epilepsy detection method based on modified recurrence plot and additive attention convolutional neural networks is proposed. In both publicly available detection tasks of epileptic EEG data, experimental results show that the method is superior and robust compared to the state-of-the-art method.

The rest of this paper is organized as follows. In Section 2, the algorithms for the construction of MRP and additive attention convolution neural network are described in detail. In Section 3, the research materials, experimental design, and results of this paper are given. In Section 4, a detailed analysis of the experimental results was presented. In Section 5, we summarize the full paper with future perspectives.

2. Mathematica method

In this paper, we propose a seizure detection method named MRP-Net. The core of MRP-Net is to extract the nonlinear features of EEG signals from phase space by constructing modified recurrent plot, and then input them into additive attention convolution neural network to automatically learn, analyze and extract the EEG features of epileptic seizures. The key to constructing modified recurrent plot is to reconstruct the EEG signal in phase space. For single-channel and multi-channel EEG signals, we use different phase space construction methods. For single-channel EEG signal, phase space reconstruction requires two key parameters: delay time τ and embedding dimension d , which are obtained by mutual information method and false nearest neighbor method respectively. For multi-channel EEG signals, we construct the phase space according to the relationship between the channels of EEG signals, and then construct modified recurrent plot. The MRP-Net method flow chart is shown in Fig. 1. It illustrates several parts of this method, which includes the preprocessing, modified recurrence plot construction, and additive attention convolution neural network module building. Then, we will introduce each part detailedly in the ensuing sections.

2.1. Phase space reconstruction

The key step in constructing a MRP is phase space reconstruction, so first we need to reconstruct the phase space of the EEG signal. In 1981, Takens [37] proposed the embedding theorem as follows: For

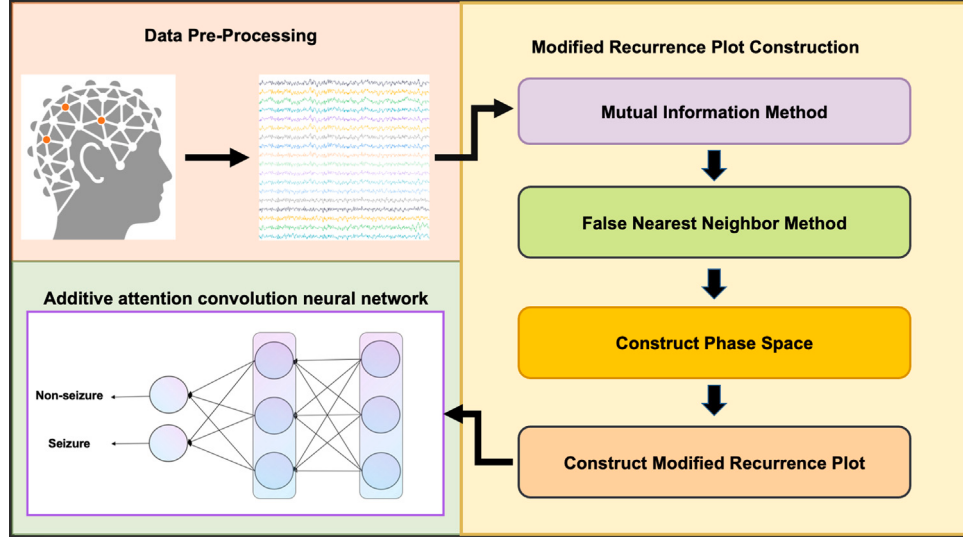


Fig. 1. The MRP-Net method flow chart.

an infinitely long, noise-free, one-dimensional, scalar time series of d' chaotic attractors, a d -dimensional embedded phase space can be found in a topologically invariant sense, provided that the dimension $d \geq 2d'$. According to Takens embedding theorem, we can reconstruct a phase space from a one-dimensional, chaotic time series in the same topological sense as the primary power system, and the determination, analysis, and prediction of the chaotic time series are performed in this reconstructed phase space. We will construct a threshold-free recurrence map based on the phase space reconstruction to extract the nonlinear features of the EEG signals of epileptic patients.

$$D_\phi = \{s_1, s_2, \dots, s_i, \dots, s_N\} \quad (1)$$

For a single-channel EEG signal time series, D_ϕ , where s_i is the observation data point at time point $i = \Delta t$ (where Δt is the sampling time) and N is the number of observations, the phase space trajectory, Eq. (2), can be reconstructed from the time series S using the time-delayed embedding method:

$$X = \{x_1, x_2, \dots, x_i, \dots, x_N | x_i = s_i, s_{i+\tau}, \dots, s_{i+(m-1)\tau}\} \quad (2)$$

where x_i is the phase point in the phase space, N is the length of the trajectory in the phase space, $N = n - (m-1)\tau$, where m is the embedding dimension, τ is the time delay and s_i is the i th data point of the EEG signal D_ϕ . Usually, the time delay and embedding dimension can be estimated from the time series S by the mutual information method [38] and the false nearest neighbor method [39,40], and we will introduce them in the next two subsections.

2.1.1. Mutual information method

Suppose there are two discrete information systems $S = \{s_1, s_2, \dots, s_m\}$ and $Q = \{q_1, q_2, \dots, q_n\}$ and their information entropy is given in Eqs. (3) and (4), respectively:

$$H(S) = - \sum_{i=1}^m P_S(s_i) \ln P_S(s_i) \quad (3)$$

$$H(Q) = - \sum_{j=1}^n P_Q(q_j) \ln P_Q(q_j) \quad (4)$$

where $P_S(s_i)$ and $P_Q(q_j)$ are the probabilities of discrete values s_i and q_j in S and Q , respectively. Then the mutual information is calculated as Eqs. (5) and (6):

$$H(S, Q) = - \sum_{i=1}^m \sum_{j=1}^n P_{S,Q}(s_i, q_j) \ln P_{S,Q}(s_i, q_j) \quad (5)$$

$$I(S, Q) = H(S) + H(Q) - H(S, Q) \quad (6)$$

Next, we will use the mutual information method to calculate the optimal time delay, as defined in Eq. (7):

$$(S, Q) = (x(i), x(i+\tau)), \quad 1 \leq i \leq n - \tau \quad (7)$$

where, S represents the time $x(i)$ and Q represents the time $x(i+\tau)$. Then $I(S, Q)$ is a function of the time delay τ , which can be written as $I(\tau)$, and the magnitude of $I(\tau)$ represents the deterministic magnitude of the $x(i+\tau)$, given the known $x(i)$. $I(\tau) = 0$ means that $x(i)$ and $x(i+\tau)$ are completely unpredictable, that is, they are completely unrelated. The minimal value of $I(\tau)$ indicates that $x(i)$ and $x(i+\tau)$ are maximally uncorrelated. The first minimal value of $I(\tau)$ is used as the optimum delay time for the phase space reconstruction. The key to the mutual information method is how to calculate the joint probability distributions $P_{S,Q}(s_i, q_j)$ and the probability distributions $P_S(s_i)$ and $P_Q(q_j)$ of S and Q systems. Our team uses the equally spaced lattice method to perform the calculations, and the method is briefly outlined below.

For Eq. (7), we use a rectangle to contain all the points on the plane (S, Q) . It is equally divided into M_S points in the S direction of the rectangle and M_Q points in the Q direction of the rectangle. (Note: usually the values of M_S and M_Q are between 100 and 200). The length of the lattice is ϵ_1 in the S direction and ϵ_2 in the Q direction. Suppose (a, b) is the vertex coordinate of the lower-left corner of the plane rectangle (S, Q) . Then start sampling the plane from (a, b) and make the following judgment on the sampling point (s, q) .

$$(i-1)\epsilon_1 \leq s - a < i\epsilon_1, \quad (j-1)\epsilon_2 \leq q - b < j\epsilon_2 \quad (8)$$

If Eq. (8) is satisfied, then it shows that (s, q) is in the lattice ϵ_{ij} and is recorded once until all data points are searched once, recording all data points N_{sq} that fall into the lattice (i, j) , the number of points N_s that fall into the range $i-1$ to i , and the number of points N_q from $j-1$ to j . Thus we can obtain Eq. (9):

$$\begin{aligned} P_S(s_i) &= N_S/N_{total} \\ P_Q(q_j) &= N_q/N_{total} \\ P_{S,Q}(s_i, q_j) &= N_{sq}/N_{total} \end{aligned} \quad (9)$$

where, N_{total} is the total number of sampling points. Substituting Eq. (9) into Eqs. (3), (4), (5), and (6), we will obtain mutual information I corresponding to the given value of τ . The detailed implementation of the mutual information method is shown in Algorithm 1.

Algorithm 1 Mutual Information Method

Require: Single-channel EEG D_ϕ , Maximum time delay τ_{max} , Number of lattices in the S and Q directions M_S, M_Q

Output: Mutual information I under the given τ

- 1: Create an empty array I to store mutual information for each τ value
- 2: Calculating the length of brainwave time series L
- 3: **for** $\tau = 0 \rightarrow \tau_{max}$ **do**
- 4: $S \leftarrow D_\phi[0, \dots, L - \tau], Q \leftarrow D_\phi[\tau, \dots, L]$
- 5: $a \leftarrow$ The minimum value in S , $b \leftarrow$ The minimum value in Q
- 6: Calculate the length of the lattice in the S and Q directions ϵ_s, ϵ_q
- 7: Create a 2-dimensional empty arrays $N_{sq}(M_S, M_Q)$ to record data points
- 8: **for** $i = 0 \rightarrow M_S$ **do**
- 9: **for** $j = 0 \rightarrow M_Q$ **do**
- 10: **for** $k = 0 \rightarrow L - \tau$ **do**
- 11: $s \leftarrow (S[k] - a)/\epsilon_s$
- 12: $q \leftarrow (Q[k] - b)/\epsilon_q$
- 13: **if** $i - 1 \leq s < i$ **and** $j - 1 \leq q < j$ **then**
- 14: $N_{sq}[i, j] \leftarrow N_{sq}[i, j] + 1$
- 15: **end if**
- 16: **end for**
- 17: **end for**
- 18: **end for**
- 19: Calculate the number of data points N_s, N_q in the S, Q direction in N_{sq} and all the number of data points N_{total}
- 20: $P_S(s_i) \leftarrow N_s/N_{total}, P_Q(q_j) \leftarrow N_q/N_{total}, P_{SQ}(s_i, q_j) \leftarrow N_{sq}/N_{total}$
- 21: Calculate the value of the mutual information I for a given value of τ
- 22: **end for**

2.1.2. False nearest neighbor method

In the previous subsection, we obtained the time delay τ , next we only need to calculate the embedding dimension m to reconstruct the phase space of the EEG signal. We will use the false nearest neighbor method to calculate the embedding dimension. Geometrically, a chaotic time series is a projection of the trajectories of chaotic motion in the high-dimensional phase space onto the one-dimensional space, and in the process of this projection, originally disjoint points may overlap; these overlapping points are called false neighbor points. In the process of phase space reconstruction, these overlapping points will be separated gradually as the embedding dimension increases, which is the false nearest neighbor method.

If the embedding dimension is m , any phase point i in the reconstructed phase space can be expressed as:

$$x_i = \{s_i, s_{i+\tau}, s_{i+2\tau}, \dots, s_{i+(m-1)\tau}\} \quad (10)$$

Assuming that the nearest phase point of x_i and x_j , the distance between the two points is:

$$D_m = \|x_i - x_j\| \quad (11)$$

where $\|\cdot\|$ represents the L2 norms. When the dimension of the phase space increases from m dimensions to $m + 1$ dimensions, the distance between two phase points is:

$$D_{m+1}^2 = \|D_m^2 + s_{i+m\tau} - s_{j+m\tau}\| \quad (12)$$

If the gap between D_m and D_{m+1} is large, it means that two nonadjacent, high-latitude, chaotic attractors become adjacent to each other when projected to lower dimensions, and therefore these two points are false neighbor points and satisfy Eq. (13)

$$\frac{\|s_{i+m\tau} - s_{j+m\tau}\|}{D_m} > D_\tau \quad (13)$$

where D_τ is the threshold value, usually $D_\tau \in [10, 50]$. For the actual chaotic sequence, the proportion of false proximity points is calculated starting from the minimum value of the embedding dimension 2, and then the dimension m is gradually increased until the proportion of false neighbor points is less than 5% or the false proximity points no longer decrease with the increase of m , at which m is the embedding dimension.

2.2. Modified recurrence plot construction

Now we have obtained the phase space of EEG signals and next we will perform a nonlinear dynamics analysis in the phase space. Recurrence plot is an effective method to visualize the nonlinear characteristics of EEG signal, which can map the trajectories of EEG waves in high-dimensional motion states to a two-dimensional plane to directly characterize its dynamical behavior and visualize the nonlinear dynamical characteristics of EEG signals. The recurrence plot is defined as follows:

$$R_{ij} = \Theta(\epsilon - D_m) \quad i, j = 1, 2, \dots, N - (m - 1)\tau \quad (14)$$

where ϵ is the distance threshold and $\Theta(\cdot)$ is the Heaviside function in Eq. (15)

$$\Theta(x) = \begin{cases} 0, & x < 0 \\ 1, & x \geq 0 \end{cases} \quad (15)$$

Although the recurrence plot can directly express the recursive characteristics of epileptic EEG signals, it loses more hidden information that cannot be recognized by the naked eye compared with the modified plot. Therefore, we change the recurrence plot method as follows:

$$R'_{ij} = \|x_i - x_j\| \quad (16)$$

where x_i and x_j are two adjacent phase points in the phase space after the reconstruction of the EEG signal in the previous subsection. In this way, a MRP containing richer nonlinear features is obtained.

Fig. 2. shows the recurrence plot and modified recurrence plot of the three physiological states of the Bonn University Dataset's single-channel EEG data, and it is observed that the recurrence plot and MRP constructed from the EEG data recorded during the normal, interictal, and seizure periods show different texture structures. Specifically, the texture gradually becomes clear and relatively compact from the normal phase to the seizure phase from blurred and sparse. Then, comparing the recurrence plot and MRP, we can see that the recurrence plot loses more hidden features that cannot be recognized by the naked eye, while the modified recurrence plot contains richer nonlinear dynamics features and retains more abstract, high-level representational property features, which can be combined with the superior feature extraction learning ability of additive attention convolution neural network.

In addition, in order to improve the generalization ability of the MRP, we changed the MRP construction method by considering the nonlinear dynamics between the multichannel EEG signals. Based on the EEG signals acquired by multiple electrodes, the phase space reconstruction process is changed as follows:

$$\begin{aligned} X' &= \{1', x_2', \dots, x_i', \dots, x_N'\} \\ x'_i &= (s_i(1)', s_i(2)', \dots, s_i(j)', \dots, s_i(n)')^T \end{aligned} \quad (17)$$

where x'_i is the phase space X' at time point i , N' and n represent the sampling length and the number of electrodes, respectively, and $s_i(j)'$ denotes the data collected by the j^{th} electrode at sampling point i . Thus, the phase space reflecting the relationship between multiple channels is obtained. Then we can construct MRP with Eq. (18)

$$D_{ij} = \|x'_i - x'_j\| \quad (18)$$

where x'_i and x'_j are two adjacent phase points in the phase space X' .

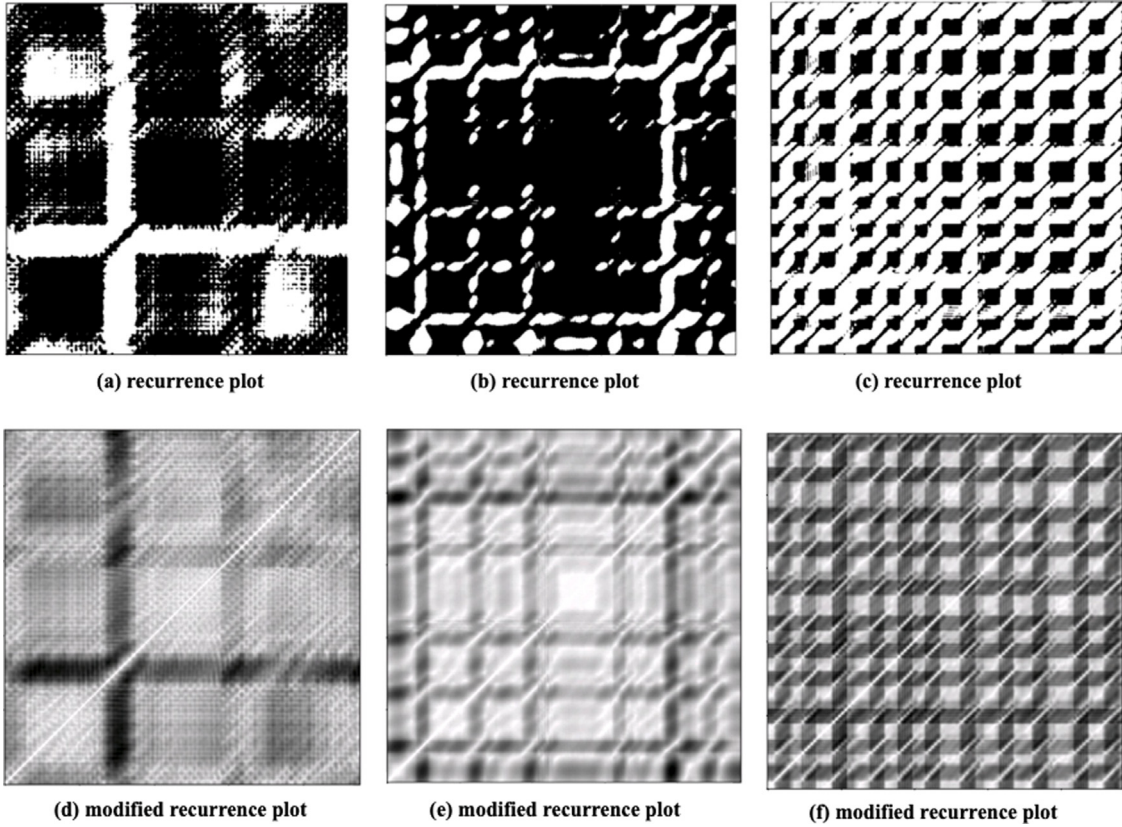


Fig. 2. Some examples of recurrence plots and modified recurrence plots constructed on the Bonn University Dataset. a, d, b, e, and c, f, correspond to the recurrence plot and modified recurrence plot constructed from the Bonn University Dataset for the EEG of normal subjects, the EEG of interictal patients, and the EEG of ictal patients, respectively.

2.3. Additive attention convolution neural network

In this paper, MPR is used to preprocess EEG signals, and a network model based on additive attention convolution neural network with residual connection is established to detect of seizures in epilepsy.

After obtaining the MRP, convolution neural network with additive attention [41] can be used to extract the underlying features layer by layer to form highly abstract high-level features and then detect seizures through fully connected neural networks.

The architecture of additive attention block is shown in Fig. 3. It first uses three independent 1×1 conv to summarize the attention matrices and transform the shape of feature maps from $H \times W \times C$ to $HW \times C/2$ as the attention query, key and value matrices $Q, K, V \in R^{N \times C/2}$, $N = H \times W$, which are written as $Q = [q_1, q_2, \dots, q_N]$, $K = [k_1, k_2, \dots, k_N]$ and $V = [v_1, v_2, \dots, v_N]$, respectively. Next, modeling the interaction between the attention query, key and value matrices. Finally, using 1×1 conv to learn global attention value and adds them with original features maps form the final output.

Specifically, the attention weight x_i of the i th query vector is computed as follows:

$$x_i = \frac{\exp(w_q^T q_i / \sqrt{C/2})}{\sum_{j=1}^N \exp(w_q^T q_j / \sqrt{C/2})} \quad (19)$$

where $w_q \in R^{C/2}$ is a learnable parameter vector. The attention query matrix is computed as follows:

$$q = \sum_{i=1}^N x_i q_i \quad (20)$$

Then use the element-wise product to compute key matrix and the attention weight y_i of the i th key vector is computed as follows:

$$x_i = \frac{\exp(w_k^T p_i / \sqrt{C/2})}{\sum_{j=1}^N \exp(w_k^T p_j / \sqrt{C/2})} \quad (21)$$

where $w_k \in R^{C/2}$ is a learnable parameter vector and the p_i is the i th vector of the global context-aware key matrix, which is formulated as follows:

$$p_i = q * k_i \quad (22)$$

where $*$ means element-wise product. Therefore, we can compute the attention key matrix as follows:

$$k = \sum_{i=1}^N y_i p_i \quad (23)$$

Next, similar with the query-key attention interaction modeling, we also perform element-wise product between the key and value, which is computed as follows:

$$u_i = k * v_i \quad (24)$$

Finally, we apply a 1×1 conv layer to learn its hidden representation and the output is added together with the original features maps.

In addition, the deeper the number of convolution layers, the stronger the ability of CNN to extract features, and the more abundant the nonlinear dynamic features mining of MRP, so we combine the additive attention block with residual convolutional neural network model (ResNet) [42] named additive attention convolutional neural network, which is description in Table 1.

3. Experiments and result

This section presents the experimental design, results, and analysis using the MRP-Net method on two publicly available datasets, Bonn University Dataset and SWEC-ETHZ Short-term Dataset. The original EEG signal was show in (see Fig. 4)

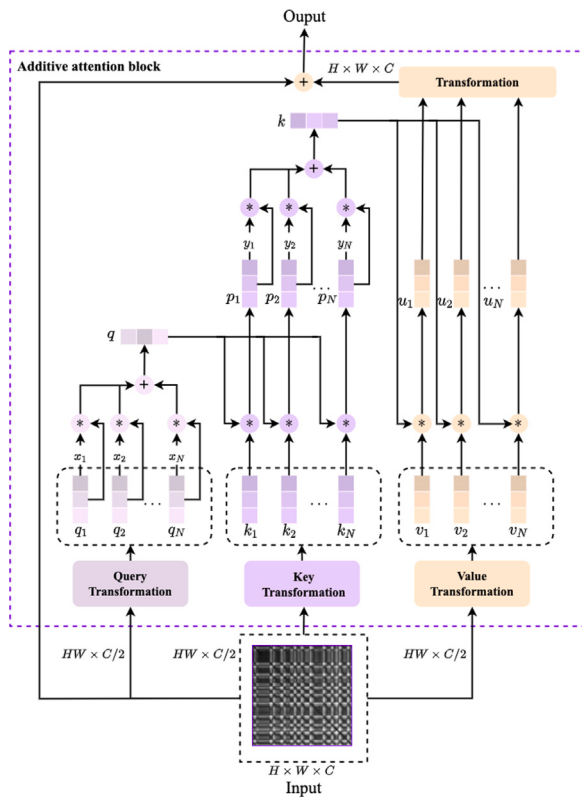


Fig. 3. The architecture of additive attention block.

3.1. Experiments dataset

3.1.1. Bonn University dataset

The Bonn University dataset [43] consists of EEG data from five healthy individuals and five patients with epilepsy and contains a total of five data subsets (A, B, C, D, E). The description of the data set is shown in Table 2. Each of these subsets contains 100 single-channel EEGs of length 23.6 s and sampling frequency 173.61 Hz, which were manually clipped from long-range multichannel EEGs. During the clipping process, some possible interferences were removed simultaneously. Subsets A and B were taken from the control group consisting of five healthy individuals. The scalp electrodes were placed as an international 10–20 system. The fragments in A are EEGs with eyes open and in B are EEGs with eyes closed. Subsets C/D/E are intracranial EEGs taken from five preoperatively diagnosed patients, and these patients have had their epilepsy fully controlled by partial hippocampal resection. The resected areas were clinically validated as epileptogenic foci. Subset C contains EEGs collected from the contralateral side of the epileptic focus, subset D contains EEGs collected from the epileptic focus, and subset E contains EEGs from intracranial electrodes. C and D were collected during the interictal period, and subset E was collected during the ictal period. Subsets C, D, and E were taken from deep electrodes. While the deep electrodes were placed, some strip electrodes were also placed in the lateral and basal regions of the neocortical layer.

3.1.2. SWEC-ETHZ Short-term Dataset

The SWEC-ETHZ Short-term Dataset included a total of 100 anonymized intracranially recorded electroencephalogram (iEEG) datasets from 16 patients with drug-resistant epilepsy who were evaluated for epilepsy surgery at the Sleep-Wake-Epilepsy Center (SWEC) of the Department of Neurology at Bern Hospital University. All patients gave written consent for their iEEG data to be used for research purposes.

Table 1

The configurations of additive attention convolution network.

Layer names	Output size	Configuration
Input layers	640 × 640 × 1	–
Conv1	320 × 320 × 64	7 × 7, stride 2
MaxPool	160 × 160 × 64	3 × 3, stride 2
Additive attention	160 × 160 × 64	–
Res1	160 × 160 × 64	[3 × 3] × 2 [3 × 3]
Res2	80 × 80 × 128	[3 × 3] × 2 [3 × 3]
Res3	40 × 40 × 256	[3 × 3] × 2 [3 × 3]
Res4	20 × 20 × 512	[3 × 3] × 2 [3 × 3]
AdaptiveAvgPool	1 × 1 × 512	–
512-d Fc, Softmax	–	–

Decisions regarding the need for iEEG recordings, electrode implantation options, and surgical treatment were made solely on a clinical basis. These decisions were made prior to and independently of the compilation of this dataset.

The iEEG signals were recorded intracranially by strip, grid, and depth electrodes (all manufactured by AD-TECH, Wisconsin, USA), using a Nicolet One recording system with a C64 amplifier (VIASYS Healthcare Inc., Madison, Wisconsin, USA). An extracranial electrode, localized between 10/20 positions Fz and Cz, was used as reference for signal recording. iEEG recordings were either sampled at 512 or 1024 Hz, depending on whether they were recorded with more or less than 64 contacts. The iEEG recorded with less than 64 contacts were down-sampled to 512 Hz prior to further analysis. iEEG signals were re-referenced against the median of all the channels free of permanent artifacts as judged by visual inspection. After 16-bit analog-to-digital conversion, the data were digitally band-pass filtered between 0.5 and 150 Hz using a fourth-order Butterworth filter prior to analysis and written onto the disk at a rate of 512 Hz. Forward and backward filtering was applied to minimize phase distortions.

All the iEEG recordings were visually inspected by an EEG board-certified experienced epileptologist (K.S.) for seizure identification and exclusion of channels continuously corrupted by artifacts. Each recording consists of 3 min of preictal segments (immediately before the seizure onset), the ictal segment (ranging from 10 s to 1002 s), and 3 min of postictal time (immediately after seizure ending). In addition to the iEEG data for each patient, the dataset includes the age, the indices of channels, the indices of resected channels, the MRI findings, the epilepsy syndrome and the post-surgical outcome. The number of electrodes per patient in the data set, the number of seizures and the duration of the seizure are described in Table 3.

3.2. Experimental settings

To validate the performance of the proposed seizure detection method based on MRP and additive attention convolution neural network, our team tested the Bonn University Dataset and SWEC-ETHZ Short-term Dataset using the MRP-Net method and compared them with state-of-the-art methods. Sensitivity Eq. (25), Specificity Eq. (26), and Accuracy Eq. (27) were used as the criteria for seizure detection to evaluate the performance of the MRP method for seizure detection.

$$\text{Sensitivity} = \frac{TP}{TP + FN} \quad (25)$$

Table 2
Description of Bonn university Dataset.

	A	B	C	D	E
Status	Eyes open	Eyes close	Interictal	Interictal	Ictal
Data type	Scalp layer	Scalp layer	Intracranial	Intracranial	Intracranial
Position	Scalp	Scalp	Seahorse structure	Focal area	Focal area
Sampling frequency(Hz)	137.61	137.61	137.61	137.61	137.61
Data points	4097	4097	4097	4097	4097

Table 3
The information of SWEC-ETHZ Short-term Dataset.

Patients ID	Number of electrodes	Number of seizures	Seizure duration(s)		
			Mean	Min	Max
1	100	5	14	10	22
2	64	4	146	89	179
3	62	14	98	31	139
4	42	4	223	96	301
5	59	6	88	67	117
6	36	2	15	14	16
7	74	7	587	154	1002
8	61	3	121	52	184
9	92	7	79	19	100
10	47	13	71	10	252
11	59	2	57	52	61
12	54	10	99	80	154
13	98	2	99	73	125
14	49	10	45	23	93
15	56	9	144	104	198
16	64	2	109	83	135

Sensitivity indicates the proportion of correctly classified positive samples.

$$\text{Specificity} = \frac{TN}{TN + FP} \quad (26)$$

Specificity indicates the proportion of correctly classified negative samples.

$$\text{Accuracy} = \frac{TP + TN}{TN + FP + FN + TP} \quad (27)$$

Accuracy indicates the proportion of correctly classified all samples.

Moreover, since the amount of data recorded in the dataset is not sufficient to train a deep network model, the available EEG data, although allowing the model to learn, suffers from significant overfitting. Acquiring a large number of EEG signals is impractical, and labeling them by neurologists is not an easy task. To overcome this difficulty, we propose a data-augmentation scheme to train our model.

In this paper, the sliding window approach [44,45] is used to increase the amount of data. Zhang et al. [45] use a sliding window size of 512 and a step size of 480 to increase the data, but a large span with a low overlap rate does not improve the performance of the model well, so, in this paper, we use an overlap rate of 80%–90% to increase the amount of our data. As shown in Fig. 5, to traverse the whole dataset in the form of dividing windows, this will greatly increase our data volume and mitigate the overfitting of the model due to insufficient data volume.

3.3. Experimental results

3.3.1. Experiments on Bonn University dataset

To maintain the high performance and efficiency of epilepsy detection, a sliding window size of 500 and a step size of 100 were chosen in Bonn University Dataset to construct MRP for single-channel EEG signals with nonlinear dynamics analysis, and then 3600 MRPs were finally obtained for each set. In addition, in order to better evaluate the performance of the proposed algorithm, seven epilepsy detection tasks were performed, including: Task (1) detection of set A and set E (normal and seizure periods, respectively); Task (2) detection of set B and set E (normal and seizure periods, respectively); Task (3) detection of set

C and set E (interictal and seizure periods, respectively); Task (4) detection of set D and set E (interepisode and episode, respectively); Task (5) detection of set A, B and set E (normal and episode, respectively); Task (6) detection of set C, D and set E (interepisode and episode, respectively); Task (7) detection of set A, B, C, D and set E (nonepisodic and episode, respectively).

In order to ensure the reliability and stability of the performance evaluation of the proposed algorithm, our team first randomly disrupted the samples and used the tenfold cross-validation method to randomly divide the MRP constructed from the single-channel EEG signals in each detection task into ten groups, each group containing the same number of MRP, nine of which were used for training and the remaining one group for testing, while traversing all the data until each group is tested once. The average of the 10 results is taken as the final detection performance.

3.3.2. Experiments on SWEC-ETHZ Short-term Dataset

From Table 3, we can find that the seizure time, number of seizures, and the number of channels of acquired signals are different for each patient of SWEC-ETHZ Short-term Dataset. Therefore, in order to capture the nonlinear characteristics between multiple channels of EEG signals and to train the deep residual network by combining the data of all patients, the phase space reconstruction is adjusted and then the multivariate thresholdless recurrence plot is constructed to accommodate different types of EEG data.

First, in order to reduce the consumption of computational resources and increase the amount of data for training, our team resampled the EEG signal to 64 Hz, then used the data collected before each patient's seizure as the interictal category and the seizure time period as the seizure category. In order to make the results more convincing and valid, the team randomly disrupted the MRP and then performed a tenfold cross-validation experiment. As the seizure onset time of each patient in the SWEC-ETHZ Short-term Dataset starts at the third minute and ends at the last three minutes of recording, as shown in Table 3, the onset times of seizures vary among patients. Therefore, when dividing the dataset into ten-fold cross-validation training and testing sets, we divided all 100 seizures for each patient into 10 folds, with each fold containing 10 seizures. A greedy algorithm was utilized

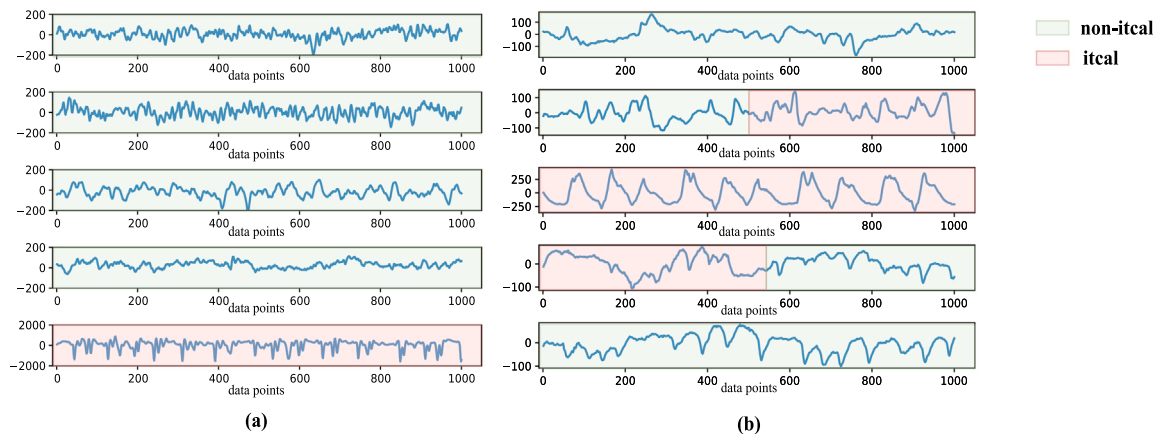


Fig. 4. The original EEG signal visualization. (a) Visualization of the original EEG signal in Bonn University Dataset five sets. (b) Visualization of the five periods(preictal period, preictal-ictal transition period, ictal period, ictal-postictal transition period, postictal period) original EEG signal from one of the patients in the SWEC-ETHZ short-term dataset, with the red region representing the ictal period and the blue region representing the non-ictal period.

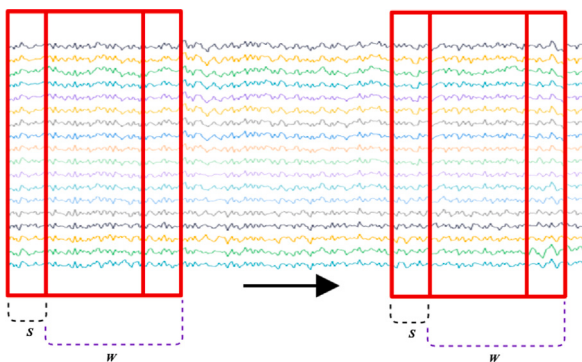


Fig. 5. The sliding-window method used in this paper, where W represents the sliding window size and S is the step size. In the experiments, a sliding window with a corresponding overlap rate of 0.9 is used to increase the amount of data.

to minimize the difference in seizure onset times between the folds. Subsequently, sliding windows with a size of 64 and a step of 10 s were applied to perform data augmentation on both the seizure and pre-seizure areas. This generated 28,877 MRPs, with 17,100 for the pre-seizure area and 11,777 for the seizure area. To maintain a balance between positive and negative samples and ensure equal data volume in each fold, we randomly discarded a portion of pre-seizure MRPs. Ultimately, we obtained 23,550 MRPs, with a ratio of seizures to pre-seizure areas equal to 11,177:11,173, and 2,355 MRPs in each fold. This data processing method effectively mitigates the issues of insufficient training data and an imbalance of positive and negative samples while preserving the independence between training and testing data. The results of the tenfold cross-validation experiment are shown in [Table 6](#). The average sensitivity, specificity, and accuracy reached 99.77%, 99.57%, and 99.69%, respectively. To explore this in more depth, we use t-SNE [46] to visualize the tenfold validation set original and trained with MRP-Net method features distribution and show it in [Fig. 6](#). As show in figure, the blue points represent seizure features and yellow points represent no-seizure features and the original indistinguishable features can be well delineated after MRP-Net method training.

Tables 4 and 5 show the results of the proposed algorithm based on this paper for seven epilepsy detection tasks on Bonn University Dataset using tenfold cross-validation method. Both single subset and multisubset detection tasks entail a two-class classification between non-seizure and a clearly defined type of seizure. Single subset detection entails using only one of the non-seizure subsets (A, B, C, or D) from the Bonn University Dataset in combination with the well-defined

type of seizure (E) from the same dataset. Multisubset detection, a task involving multiple subsets of non-epileptic seizures (AB, CD, or ABCD), combined with the well-defined type of seizure (E). The proposed algorithm achieves 100% results in sensitivity, specificity, and accuracy for the seven seizure detection tasks on Bonn University Dataset. In order to further validate the superiority of the EEG seizure detection based on the algorithm in this paper, the results are also compared with other state-of-the-art methods using the same dataset, and the comparison results are also presented in Tables.

4. Discussion

In this work, this paper proposes the use of MRP for nonlinear dynamics analysis of EEG signals to detect seizures and employs an additive attention convolution neural network to train the training set to extract more high-level, abstract, nonlinear cryptic features. All the data can be directly constructed as MRP after preprocessing. The construction of the MRP is the key to produce excellent results, which can visualize the nonlinear features of the EEG signal during seizures. In addition, in order to make the MRP algorithm more generalizable, we extended the MRP algorithm to adapt it to work with multichannel EEG signals. The two publicly available evaluation datasets and evaluation metrics used in this study are detailed in Sections 3.1 and 3.2. To better evaluate the performance of the proposed algorithm in this paper, we compared the results with other research works.

The results of the Bonn University Dataset comparison experiments used in this paper are shown in [Tables 4](#) and [5](#). The Bonn University Dataset has been used in many seizure detection studies, and it is valid and feasible to use it to evaluate the proposed seizure detection algorithm and compare the proposed algorithm with other existing work. [Table 4](#) presents the sensitivity, specificity, and accuracy of the four single-subset seizure detection tasks performed in this paper compared to previous work. In the first four, single-subset A, B, C, D (no seizures) and subset E (seizures) detection tasks, researchers have been working for a long time to detect seizures using a combination of manual feature extraction and traditional machine-learning algorithms. The accuracy of these methods ranged from 93% to 99.85%, among which Fu et al. [54] used Hilbert's marginal spectrum (HMS) to analyze the EEG signal considering the nonlinearity and nonstationarity of the EEG signal, and then input it into SVM for classification to achieve the highest accuracy of 99.85% in the detection task of subsets A and E. In recent years, Peng et al. [55] proposed a novel homologous dictionary learning (DLWH)-based epilepsy detection algorithm that outperformed previous work in both the detection tasks of single subsets A, B, C, D (no seizures) and subset E (seizures), especially in the detection tasks of subsets A and E. Sensitivity, specificity, and accuracy were all 100%. However,

Table 4

Comparison of performance of proposed method with other methods in single subset detection tasks.

Task	Ref.	Methods	Sensitivity(%)	Specificity(%)	Accuracy(%)
A vs E.	Saastamoinen et al. [47]	Time-frequency domain feature, radial basis function (RBF)	–	–	97.2
	Polat and Günes [48]	FFT-decision tree classifier	99.4	99.31	98.72
	Subasi [49]	Discrete wavelet transform (DWT), mixture of expert model	95	94	95
	Guo et al. [50]	DWT-relative wavelet energy, MLP	98.17	92.12	95.2
	Wang et al. [51]	Wavelet transform and Shannon entropy, (K Nearest Neighbor) KNN	–	–	99.45
	Nicoletta et al. [52]	Permutation entropy, SVM	–	–	93.55
	Fu et al. [53]	Hibert-Huang transform (HHT), SVM	–	–	99.13
	Fu et al. [54]	HMS analysis, SVM	–	–	99.85
	Peng et al. [55]	DLWH	100	100	100
	Ours	MRP-Net	100	100	100
B vs E.	Supriya et al. [56]	Weighted visibility graph and SVM	–	–	97.25
	Peng et al. [55]	DLWH	100	95	97.5
	Ours	MRP-Net	100	100	100
C vs E.	Samiee et al. [57]	Rational discrete short-time Fourier transform and MLP	99.3	97.7	9.5
	Siuly et al. [58]	Clustering technique-based least square support vector machine (LS-SVM)	88	100	94
	Peng et al. [55]	DLWH	98	100	99
D vs E.	Ours	MRP-Net	100	100	100
	Siuly et al. [59]	Least square support vector machine (LS-SVM)	88	100	94
	Samiee et al. [57]	Rational Discrete Short Time Fourier Transform	95.6	94.1	94.9
	Kaya et al. [60]	One-dimensional local pattern (1D-LBP)	96	95	95.5
	Siuly et al. [58]	Clustering technique-based LS-SVM	89.4	97.8	93.6
D vs E.	Kumar et al. [61]	DWT and approximate entropy	94	92	93
	Peng et al. [55]	DLWH	99	100	99.5
	Ours	MRP-Net	100	100	100

Table 5

Comparison of performance of proposed method with other methods in multisubset detection tasks.

Task	Ref.	Methods	Sensitivity(%)	Specificity(%)	Accuracy(%)
AB vs E.	Ullah et al. [62]	Pyramidal one-dimensional convolutional neural network	98	99	98.2
	Sharma et al. [63]	Tunable Q-factor wavelet transform and FD and LS-SVM	–	–	100
	Sharma et al. [64]	Analytic time-frequency flexible wavelet transform,FD and LS-SVM	–	–	100
	Sharmila et al. [44]	DWT and naïve Bayes (NB) /KNN	98.02	99.74	99.16
	Ours	MRP-Net	100	100	100
	Sharma et al. [63]	Tunable Q-factor wavelet transform, FD and LS-SVM	–	–	99.67
	Sharma et al. [64]	Analytic time-frequency flexible wavelet transform,FD and LS-SVM	–	–	98.67
	Sharmila et al. [44]	DWT and NB/KNN	94.4	96.44	95.75
	Ours	MRP-Net	100	100	100
	Sharma et al. [63]	Tunable Q-factor wavelet transform and FD and LS-SVM	–	–	99.6
CD vs E.	Sharma et al. [64]	Analytic time-frequency flexible wavelet transform,FD and LS-SVM	–	–	98.67
	Sharmila et al. [44]	DWT and NB/KNN	90.88	96.25	95.25
	Siuly et al. [65]	Hermite transform and LS-SVM	–	–	97.6
	TharaD. et al. [66]	DNN	98.59	91.47	97.21
	Gupta et al. [67]	Weighted multiscale Renyi permutation entropy (WMRPE) and rhythms	–	–	98.6
ABCD vs E.	Hassan et al. [68]	CEEMDAN and normal inverse Gaussian pdf parameters and adaptive boosting	98.75	98.75	97.2
	Akyol [69]	SEA-based DNN	93.11	98.18	97.17
	Sukriti et al. [70]	Kurtosis-based VMD's parameters selection and bandwidth features	99.1	100	99.3
	Ours	MRP-Net	100	100	100

Table 6

Tenfold cross-validation experiment result on SWEC-ETHZ Short-term Dataset Dataset.

	Sensitivity (%)	Specificity (%)	Accuracy (%)
Fold 1	99.57	99.65	99.61
Fold 2	99.92	99.41	99.71
Fold 3	99.83	99.52	99.71
Fold 4	99.75	99.52	99.66
Fold 5	99.73	99.56	99.66
Fold 6	99.82	99.31	99.61
Fold 7	99.92	99.53	99.75
Fold 8	99.74	99.65	99.71
Fold 9	99.91	99.65	99.80
Fold 10	99.50	99.88	99.66
Mean	99.77	99.57	99.69

accuracy is only 97% in the detection tasks of subsets B and E, which indicates that the algorithm does not necessarily perform well in some detection tasks. And the proposed seizure detection algorithm MRP-Net in this paper achieved perfect results of 100% in the detection tasks of sensitivity, specificity, and accuracy in a single subset A, B, C, D (no seizure) and subset E (seizure). This shows that the proposed algorithm is not only more superior but also more robust. To further demonstrate

this, three additional multisubset detection tasks were performed, and the experimental comparison results are shown in **Table 5**. Sharma et al. Sharma et al. [63,64] proposed to use the nonlinear chaotic property of FD to analyze EEG signals and then applied least squares support vector machine (LS-SVM) for classification to achieve better performance in three multisubset detection tasks, especially in the detection tasks of subsets AB and E with an accuracy of 100%. TharaD. et al. [66] used DNN for epilepsy detection with sensitivity, specificity, and accuracy of 98.59%, 91.47%, and 97.21%, respectively, in the detection tasks of subsets ABCD and E, respectively. Hassan et al. [68] proposed to first decompose the fragments of EEG signals into intrinsic mode functions using the complete ensemble empirical mode decomposition of adaptive noise (CEEMDAN). Then the mode functions were modeled by normal inverse Gaussian (NIG) pdf parameters and were finally input to adaptive boosting for learning classification; they achieved good performance on the detection tasks of subsets A, B, C, D, and E. Sensitivity, specificity, and accuracy were 98.75%, 98.75%, and 99.2%, respectively. Sukriti et al. [70] proposed an automatic seizure detection method using variational pattern decomposition (VMD) and achieved excellent performance using RF classifier with sensitivity, specificity, and accuracy of 99.1%, 100%, and 99.3%, respectively. The

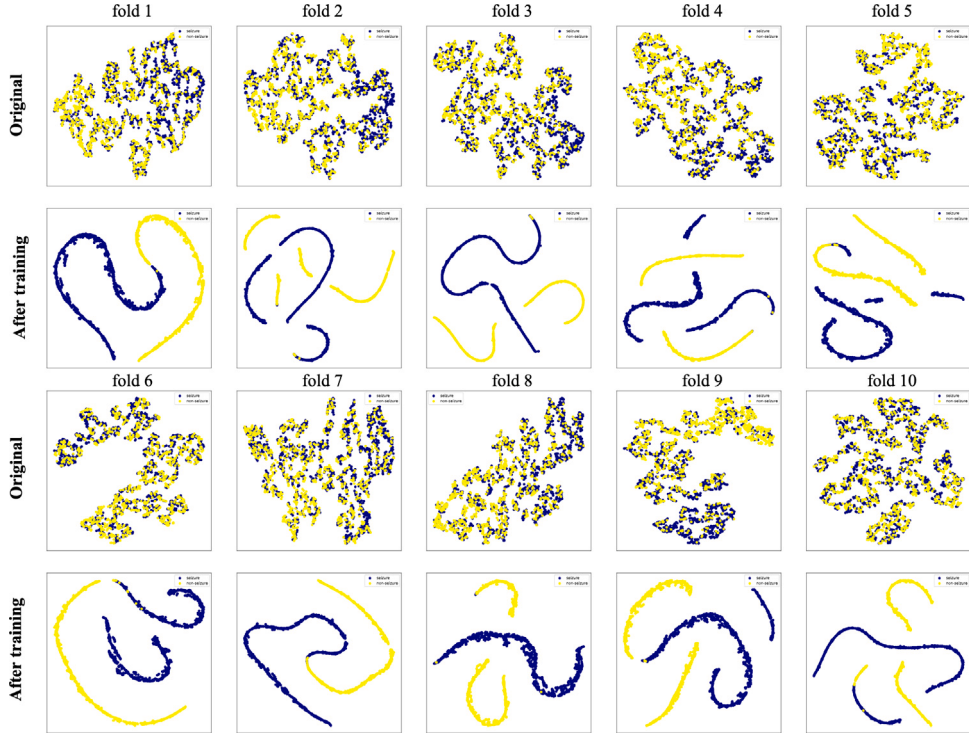


Fig. 6. Visualization distribution of data using t-SNE, the blue points represent seizure features and yellow points represent no-seizure features. The original seizure and non-seizure features are indistinguishable and after MRP-Net training the features can be well delineated.

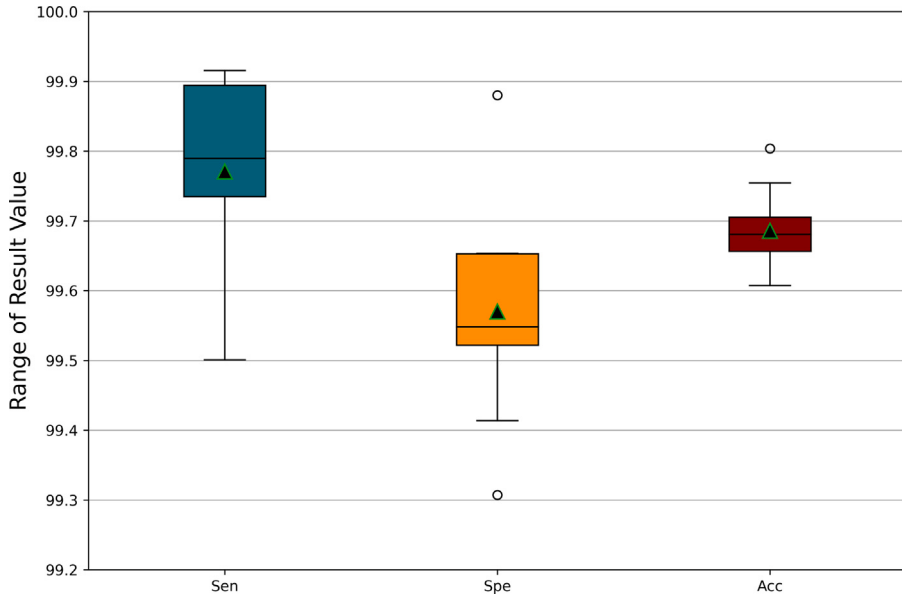


Fig. 7. The box plot shows the result of the mean sensitivity, specificity, and accuracy in tenfold cross-validation.

proposed algorithm achieved 100% results for sensitivity, specificity, and accuracy in these detection tasks, which further demonstrates the high accuracy and enhanced robustness of the proposed algorithm. In addition to these detection tasks, we only list a few of the works, which are described in detail in Tables 4 and 5.

In SWEC-ETHZ Short-term Dataset, this paper uses MRP to extract the nonlinear features of multichannel EEG signals. The detailed results of each fold after the tenfold cross-validation are shown in Table 6. In addition, Fig. 7 shows the block diagram of all experimental results representing the distribution of different indicators' results. As shown

in the figure, the proposed algorithm in this paper is more sensitive to the positive samples of the experimental data, which indicates a lower leakage rate in the practical application of automatic seizure detection and meets the realistic application value. Since the SWEC-ETHZ Short-term Dataset is an epilepsy EEG dataset released in recent years, we only compared the work of the original dataset paper in the comparison experiments. The comparison results are shown in Fig. 8. Burrello et al. [11] proposed a fast-learning method combining symbolic dynamics and brain-inspired, high-latitude computation for each patient-specific learning with a macroscopic average accuracy of 95.42% to achieve

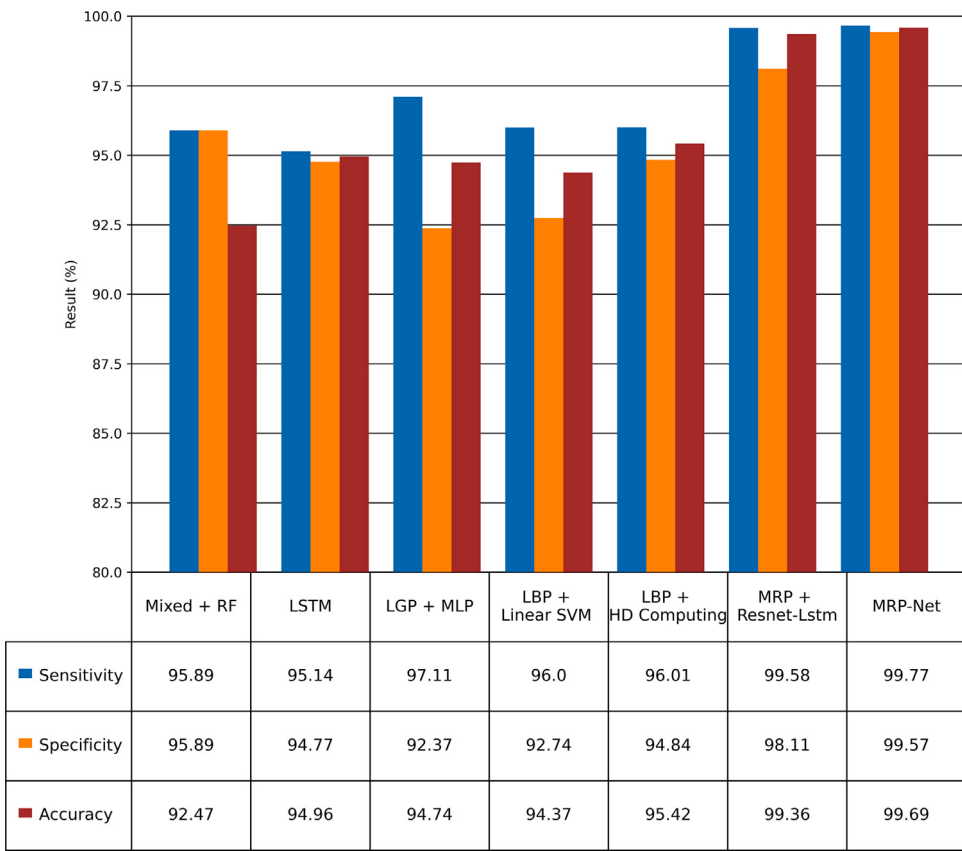


Fig. 8. Performance comparison with other state-of-the-art method.

superior results. In contrast, the method proposed in this paper can fully take into account the nonlinear relationship between different channels and eliminate the limitation existing in the different number of channels of the data itself, which can be adapted to different patients. The classification average accuracy reaches 99.69%, compared with which the seizure detection accuracy of the algorithm proposed in this paper is improved by 4.27%. In addition, we also set up a group of comparative experiments on the combination of CNN and RNN. Specifically, we build a Resnet-Lstm model that contains Resnet18 and two layers of LSTM layers with hidden dimensions of 128. After inputting MRP into the model, firstly, the image features of MRP are extracted by Resnet18, and then the feature vectors are input into LSTM for prediction. The experimental results are as shown by Fig. 8, Resnet-Lstm model also has superior prediction ability, slightly inferior to MRP-Net. According to our analysis, because MRP-Net and Resnet-Lstm backbone are the same, but the difference lies in the additive attention and LSTM layers, additive attention can improve the performance of the model by making the model focus on the important features in the input data and capture the long-term dependence between the data. Although LSTM can also capture long-term dependence, it acts after Resnet18 feature extraction. Obviously, its effect may not be as effective as using additive attention to capture long-term dependence before Resnet18 feature extraction.

To further illustrate the effectiveness of the proposed algorithm in this paper for nonlinear feature extraction of seizure EEG signals, we visualized some feature maps of the MRP after automatic extraction by the additive attention convolution neural network. As shown in Fig. 9, initially the network layers extracted primary texture features, which effectively preserved the overall contour of the MRP, and then the comparison revealed that with the gradual increase of the network layers. The feature map reflected rich texture detail information, which was the extraction of the original MRP detail features with more advanced features that could hardly be clearly identified with the naked

eye and fully exploited the nonlinear occultation features of the MRP. It can be seen that the proposed algorithm in this paper effectively mines and learns the nonlinear dynamics features of the epileptic EEG signal, and thus obtains a high detection accuracy.

Overall, although simpler machine learning algorithms have shown good results in detecting seizures, the variability and non-stationarity of the EEG signal means that the EEG is highly variable across individuals at different times, and these factors can pose significant challenges to machine learning algorithms and may lead to misclassification or low accuracy. By using more sophisticated algorithms, such as deep neural networks, researchers can potentially address some of these limitations and achieve higher classification performance. These algorithms aim to extract highly abstract and discriminative features from the EEG signal that may be difficult to detect by other machine learning models. Therefore, the MRP-Net algorithm proposed in this paper is relatively complex but it achieves excellent performance and is more robust. The reasons are firstly, MRP can effectively extract the nonlinear hidden features of EEG signals, secondly, Additive attention convolution neural network can extract highly abstract and discriminative features from MRP, and thirdly, sliding window data enhancement can effectively alleviate the data dependence of deep neural network.

Furthermore, currently, the majority of studies on detecting seizures [4,8,46,50–70] have mainly focused on classifying interictal and ictal states. However, detecting preictal conditions from the interictal period is of greater clinical value, and this is also one of the limitations of this article. However, accurately identifying and predicting preictal states is challenging because these states tend to exhibit highly variable and nonlinear patterns in EEG data [20–22], making preictal states diverse and constantly changing. Detecting preictal states is an important goal that requires further research to develop reliable and accurate models.

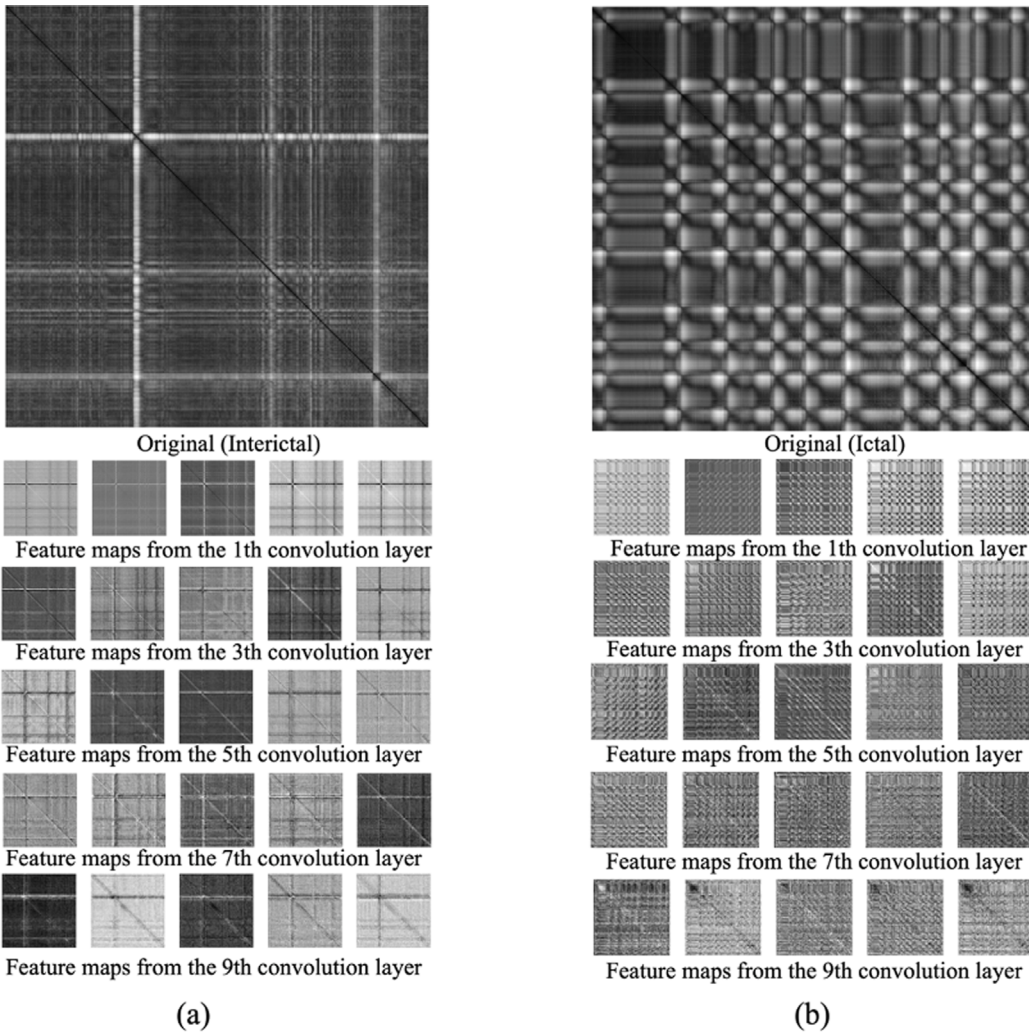


Fig. 9. Some examples of additive attention convolution neural network feature maps for feature extraction in SWEC-ETHZ Short-term Dataset. (a) and (b) original images are MRP constructed from multichannel EEG signals during the interictal and ictal phases.

5. Conclusion

In this paper, a novel nonlinear analysis method, MRP-Net, has been proposed for EEG seizure detection. In the proposed method, the MRP and an additive attention convolution neural network are proposed to be combined for feature extraction and classification. The nonlinear dynamics features have been extracted by introducing the MRP method from EEG signals, and the MRPs have been input to an additive attention convolution neural network by introducing the module to automatically learn, extract, and analyze the nonlinearity and nonstationarity of seizures. Finally, the proposed method has been subjected to several validation experiments on two publicly available epileptic EEG datasets. The experimental results have been showed that the proposed algorithm has been improved accuracy in seizure detection compared to previous work. By fully exploiting the nonlinear cryptic features of the EEG signal, the impact of neglecting the nonlinearity and nonsmoothness of the EEG signal on the detection accuracy is effectively mitigated, providing an effective scheme for nonlinear kinetic analysis of seizure detection. In addition, although the MRP-Net has achieved excellent performance in epilepsy detection, it still deserves further research, especially for the performance of the MRP-Net method in areas such as EEG motor imagery classification and emotion recognition. The nonlinearity and nonsmoothness features of motor imagery and emotion can also be extracted with the MRP method and classified with the additive attention neural network. Our team will

further investigate the MRP-Net performance in various types of EEG signals.

CRediT authorship contribution statement

Wenkai Huang: Conceptualization, Supervision, Writing – review & editing. **Haizhou Xu:** Data curation, Methodology, Software, Writing – original draft. **Yujia Yu:** Validation, Visualization, Investigation.

Declaration of competing interest

The authors declare that they have no known competing financial interests or personal relationships that could have appeared to influence the work reported in this paper.

Data availability

No data was used for the research described in the article.

Acknowledgment

The work was supported by Guangzhou Youth Science and Technology Education Project (No. KP2023243 & KP2023245).

References

- [1] U.R. Acharya, S.V. Sree, G. Swapna, R.J. Martis, J.S. Suri, Automated EEG analysis of epilepsy: A review, *Knowl.-Based Syst.* 45 (2013) 147–165.
- [2] D. Gajic, D. Gajic, Z. Djurovic, S.D. Gennaro, F.K. Gustafsson, Classification of EEG signals for detection of epileptic seizures based on wavelets and statistical pattern recognition, *Biomed. Eng.: Appl., Basis Commun.* 26 (2014) 1450021.
- [3] T.S. Kumar, V. Kanhangad, R.B. Pachori, Classification of seizure and seizure-free EEG signals using local binary patterns, *Biomed. Signal Process. Control.* 15 (2015) 33–40.
- [4] S. Aydin, H.M. Saraoğlu, S. Kara, Log energy entropy-based EEG classification with multilayer neural networks in seizure, *Ann. Biomed. Eng.* 37 (2009) 2626–2630.
- [5] C. Ieracitano, J. Duun-Henriksen, N. Mammone, F.L. Foresta, F.C. Morabito, Wavelet coherence-based clustering of EEG signals to estimate the brain connectivity in absence epileptic patients, in: 2017 International Joint Conference on Neural Networks, IJCNN, 2017, pp. 1297–1304.
- [6] T. Zhang, W. Chen, LMD based features for the automatic seizure detection of EEG signals using SVM, *IEEE Trans. Neural Syst. Rehabil. Eng.* 25 (2017) 1100–1108.
- [7] M. Mursalin, Y. Zhang, Y. Chen, N. Chawla, Automated epileptic seizure detection using improved correlation-based feature selection with random forest classifier, *Neurocomputing* 241 (2017) 204–214.
- [8] S. AYDIN, Comparison of power spectrum predictors in computing coherence functions for intracortical EEG signals, *Ann. Biomed. Eng.* 37 (1) (2009) 192–200.
- [9] S. Aydin, Determination of autoregressive model orders for seizure detection, *Turk. J. Electr. Eng. Comput. Sci.* 18 (1) (2010) 23–30.
- [10] L. Vidyaratne, K.M. Iftekharuddin, Real-time epileptic seizure detection using EEG, *IEEE Trans. Neural Syst. Rehabil. Eng.* 25 (2017) 2146–2156.
- [11] A. Burrello, K.A. Schindler, L. Benini, A. Rahimi, Hyperdimensional computing with local binary patterns: One-shot learning of seizure onset and identification of Ictalogenic Brain Regions using short-time iEEG recordings, *IEEE Trans. Biomed. Eng.* 67 (2020) 601–613.
- [12] Y. Bengio, A.C. Courville, P. Vincent, Representation learning: A review and new perspectives, *IEEE Trans. Pattern Anal. Mach. Intell.* 35 (2013) 1798–1828.
- [13] U.R. Acharya, S.L. Oh, Y. Hagiwara, J.H. Tan, H. Adeli, Deep convolutional neural network for the automated detection and diagnosis of seizure using EEG signals, *Comput. Biol. Med.* 100 (2018) 270–278.
- [14] X. mei Hu, S. Yuan, F. Xu, Y. Leng, K. Yuan, Q. Yuan, Scalp EEG classification using deep Bi-LSTM network for seizure detection, *Comput. Biol. Med.* 124 (2020) 103919.
- [15] Y. Zhao, C. Dong, G. Zhang, Y. Wang, X. Chen, W. Jia, Q. Yuan, F. Xu, Y. Zheng, EEG-based seizure detection using linear graph convolution network with focal loss, *Comput. Methods Programs Biomed.* 208 (2021) 106277.
- [16] M.D. Woodbright, B.K. Verma, A. Haidar, Autonomous deep feature extraction based method for epileptic EEG brain seizure classification, *Neurocomputing* 444 (2021) 30–37.
- [17] T. McKenna, T. McMullen, M.F. Shlesinger, The brain as a dynamic physical system, *Neuroscience* 60 (1994) 587–605.
- [18] D. Garrett, D.A. Peterson, C.W. Anderson, M.H. Thaut, Comparison of linear, nonlinear, and feature selection methods for EEG signal classification, *IEEE Trans. Neural Syst. Rehabil. Eng.* 11 (2003) 141–144.
- [19] K. Natarajan, R.A. U, F. Alias, T. Tiboleng, S. Puthusserypady, Nonlinear analysis of EEG signals at different mental states, *BioMed. Eng. OnLine* 3 (2004) 7.
- [20] Y. Zhang, W. Zhou, S. Yuan, Q. Yuan, Seizure detection method based on fractal dimension and gradient boosting, *Epilepsy Behav.* 43 (2015) 30–38.
- [21] B.D. Chalageri, R. Halima, H. Nagendra, Epileptic seizure detection using an algorithm based on fractal dimension, *Int. J. Eng. Res.* 5 (2016) 26–29.
- [22] Q.D.K. Truong, N.T.M. Huong, V.V. Toi, Detecting epileptic seizure from scalp EEG using Lyapunov spectrum, *Comput. Math. Methods Med.* 2012 (2012).
- [23] F. Shayegh, S. Sadri, R. Amirfattahi, K. Ansari-Asl, A model-based method for computation of correlation dimension, Lyapunov exponents and synchronization from depth-EEG signals, *Comput. Methods Programs Biomed.* 113 1 (2014) 323–337.
- [24] A.Q. Rincón, M. Flugelman, J. Prendes, C. d'Giano, Study on epileptic seizure detection in EEG signals using largest Lyapunov exponents and logistic regression, *Rev. Argentina Bioingeniería* 23 (2) (2019) 17–24.
- [25] A. Gupta, P. Singh, M. Karlekar, A novel signal modeling approach for classification of seizure and seizure-free EEG signals, *IEEE Trans. Neural Syst. Rehabil. Eng.* 26 (2018) 925–935.
- [26] S. Lahmri, A. Shmuel, Accurate classification of seizure and seizure-free intervals of intracranial EEG signals from epileptic patients, *IEEE Trans. Instrum. Meas.* 68 (2019) 791–796.
- [27] L. Hussain, S. Saeed, I.A. Awan, A. Idris, Multiscaled complexity analysis of EEG epileptic seizure using entropy-based techniques, *Arch. Neurosci.* 5 (2018).
- [28] K. Zeng, G. Ouyang, H. Chen, Y. Gu, X. Liu, X. Li, Characterizing dynamics of absence seizure EEG with spatial-temporal permutation entropy, *Neurocomputing* 275 (2018) 577–585.
- [29] T. Zhang, W. Chen, M. Li, Complex-valued distribution entropy and its application for seizure detection, *Biocybern. Biomed. Eng.* 40 (2020) 306–323.
- [30] N. Thomasson, T.J. Hoeppner, C.L. Webber, J.P. Zbilut, Recurrence quantification in epileptic EEGs, *Phys. Lett. A* 279 (2001) 94–101.
- [31] U.R. Acharya, S.V. Sree, S. Chattopadhyay, W. Yu, P.C.A. Ang, Application of recurrence quantification analysis for the automated identification of epileptic EEG signals, *Int. J. Neural Syst.* 21 3 (2011) 199–211.
- [32] B. Akbarian, A. Erfanian, Automatic seizure detection based on nonlinear dynamical analysis of EEG signals and mutual information, *Basic Clin. Neurosci.* 9 (2018) 227–240.
- [33] J.-P. Eckmann, S.O. Kamphorst, D. Ruelle, Recurrence plots of dynamical systems, *Europhys. Lett.* 4 (1987) 973–977.
- [34] D. Wang, Y. Guo, X. Wu, J. Na, G. Litak, Planetary-gearbox fault classification by convolutional neural network and recurrence plot, *Appl. Sci.* 10 (2020) 932.
- [35] F.O. Ozkok, M. Celik, Convolutional neural network analysis of recurrence plots for high resolution melting classification, *Comput. Methods Programs Biomed.* 207 (2021) 106139.
- [36] X. Meng, S. Qiu, S. Wan, K. Cheng, L. Cui, A motor imagery EEG signal classification algorithm based on recurrence plot convolution neural network, *Pattern Recognit. Lett.* 146 (2021) 134–141.
- [37] F. Takens, Detecting strange attractors in turbulence, in: *Dynamical Systems and Turbulence*, Warwick 1980, Springer, 1981, pp. 366–381.
- [38] Fraser, Swinney, Independent coordinates for strange attractors from mutual information, *Phys. Rev. A. General Phys.* 33 2 (1986) 1134–1140.
- [39] Kennel, Brown, Abarbanel, Determining embedding dimension for phase-space reconstruction using a geometrical construction, *Phys. Rev. A, At., Mol. Opt. Phys.* 45 6 (1992) 3403–3411.
- [40] L. Cao, Practical method for determining the minimum embedding dimension of a scalar time series, *Physica D* 110 (1997) 43–50.
- [41] C. Wu, F. Wu, T. Qi, Y. Huang, Fastformer: Additive attention can be all you need, 2021, ArXiv, arXiv:2108.09084.
- [42] K. He, X. Zhang, S. Ren, J. Sun, Deep residual learning for image recognition, in: 2016 IEEE Conference on Computer Vision and Pattern Recognition, CVPR, 2016, pp. 770–778.
- [43] R.G. Andrzejak, K. Lehnertz, F. Mormann, C. Rieke, P. David, C.E. Elger, Indications of nonlinear deterministic and finite-dimensional structures in time series of brain electrical activity: Dependence on recording region and brain state., *Phys. Rev. E, Stat., Nonlinear, Soft Matter Phys.* 64 6 Pt 1 (2001) 061907.
- [44] A. Sharmila, P. Geethanjali, DWT based detection of epileptic seizure from EEG signals using naive Bayes and k-NN classifiers, *IEEE Access* 4 (2016) 7716–7727.
- [45] T. Zhang, W. Chen, M. Li, AR based quadratic feature extraction in the VMD domain for the automated seizure detection of EEG using random forest classifier, *Biomed. Signal Process. Control.* 31 (2017) 550–559.
- [46] L. van der Maaten, G.E. Hinton, Visualizing data using t-SNE, *J. Mach. Learn. Res.* 9 (2008) 2579–2605.
- [47] A. Saastamoinen, T. Pietilä, A. Värrä, M. Lehtokangas, J. Saarinen, Waveform detection with RBF network - application to automated EEG analysis, *Neurocomputing* 20 (1998) 1–13.
- [48] K. Polat, S. Günes, Classification of epileptiform EEG using a hybrid system based on decision tree classifier and fast Fourier transform, *Appl. Math. Comput.* 187 (2007) 1017–1026.
- [49] A. Subasi, EEG signal classification using wavelet feature extraction and a mixture of expert model, *Expert Syst. Appl.* 32 (2007) 1084–1093.
- [50] L. Guo, D. Rivero, J.A. Seoane, A. Pazos, Classification of EEG signals using relative wavelet energy and artificial neural networks, in: Proceedings of the First ACM/SIGEVO Summit on Genetic and Evolutionary Computation, 2009, pp. 177–184.
- [51] D. Wang, D. Miao, C. Xie, Best basis-based wavelet packet entropy feature extraction and hierarchical EEG classification for epileptic detection, *Expert Syst. Appl.* 38 (2011) 14314–14320.
- [52] N. Nicolaou, J. Georgiou, Detection of epileptic electroencephalogram based on permutation entropy and support vector machines, *Expert Syst. Appl.* 39 (2012) 202–209.
- [53] K. Fu, J. Qu, Y. Chai, Y. Dong, Classification of seizure based on the time-frequency image of EEG signals using HHT and SVM, *Biomed. Signal Process. Control.* 13 (2014) 15–22.
- [54] K. Fu, J. Qu, Y. Chai, T. Zou, Hilbert marginal spectrum analysis for automatic seizure detection in EEG signals, *Biomed. Signal Process. Control.* 18 (2015) 179–185.
- [55] H. Peng, C. Li, J. Chao, T. Wang, C. Zhao, X. Huo, B. Hu, A novel automatic classification detection for epileptic seizure based on dictionary learning and sparse representation, *Neurocomputing* 424 (2021) 179–192.
- [56] Supriya, S. Siuly, H. Wang, J. Cao, Y. Zhang, Weighted visibility graph with complex network features in the detection of epilepsy, *IEEE Access* 4 (2016) 6554–6566.
- [57] K. Samiee, P. Kovács, M. Gabbouj, Epileptic seizure classification of EEG time-series using rational discrete short-time Fourier transform, *IEEE Trans. Biomed. Eng.* 62 (2015) 541–552.
- [58] S. Siuly, Y. Li, P. Wen, Clustering technique-based least square support vector machine for EEG signal classification, *Comput. Methods Programs Biomed.* 104 3 (2011) 358–372.

- [59] Siuly, Y. Li, P. Wen, EEG signal classification based on simple random sampling technique with least square support vector machine, *Int. J. Biomed. Eng. Technol.* 7 (2011) 390.
- [60] Y. Kaya, M. Uyar, R. Tekin, S. Yildirim, 1D-local binary pattern based feature extraction for classification of epileptic EEG signals, *Appl. Math. Comput.* 243 (2014) 209–219.
- [61] Y. Kumar, M.L. Dewal, R.S. Anand, Epileptic seizures detection in EEG using DWT-based ApEn and artificial neural network, *Signal, Image Video Process.* 8 (2014) 1323–1334.
- [62] I. Ullah, M. Hussain, E. ul Haq Qazi, H.A. Aboalsamh, An automated system for epilepsy detection using EEG brain signals based on deep learning approach, 2018, ArXiv [arXiv:1801.05412](https://arxiv.org/abs/1801.05412).
- [63] M.K. Sharma, R.B. Pachori, A novel approach to detect epileptic seizures using a combination of tunable-Q wavelet transform and fractal dimension, *J. Mech. Med. Biol.* 17 (2017) 1740003.
- [64] M.K. Sharma, R.B. Pachori, U.R. Acharya, A new approach to characterize epileptic seizures using analytic time-frequency flexible wavelet transform and fractal dimension, *Pattern Recognit. Lett.* 94 (2017) 172–179.
- [65] S. Siuly, O.F. Alcin, V. Bajaj, A. Şengur, Y. Zhang, Exploring Hermite transformation in brain signal analysis for the detection of epileptic seizure, *IET Sci., Meas. Technol.* (2019).
- [66] K. TharaD., G. PremaSudhaB., F. Xiong, Auto-detection of epileptic seizure events using deep neural network with different feature scaling techniques, *Pattern Recognit. Lett.* 128 (2019) 544–550.
- [67] V. Gupta, R.B. Pachori, Epileptic seizure identification using entropy of FBSE based EEG rhythms, *Biomed. Signal Process. Control.* 53 (2019).
- [68] A.R. Hassan, A. Subasi, Y. Zhang, Epilepsy seizure detection using complete ensemble empirical mode decomposition with adaptive noise, *Knowl.-Based Syst.* 191 (2020) 105333.
- [69] K. Akyol, Stacking ensemble based deep neural networks modeling for effective epileptic seizure detection, *Expert Syst. Appl.* 148 (2020) 113239.
- [70] Sukriti, M. Chakraborty, D. Mitra, Epilepsy seizure detection using kurtosis based VMD's parameters selection and bandwidth features, *Biomed. Signal Process. Control.* 64 (2021) 102255.